Magnetically activated electroactive microenvironments for skeletal muscle tissue regeneration

Sylvie Ribeiro[1,2], Clarisse Ribeiro[1,3,*], Estela O. Carvalho[1,3], Carmen R. Tubio[4], Nelson Castro[4], N. Pereira[1,5], Vitor Correia[1,5], Andreia C. Gomes[2] and Senentxu Lanceros-Méndez[1,4,6]

[1]Centro/Departamento de Física, Universidade do Minho, Campus de Gualtar, 4710-057 Braga, Portugal;

[2]Centre of Molecular and Environmental Biology (CBMA), Universidade do Minho, Campus de Gualtar, 4710-057 Braga, Portugal;

[3]CEB—Centre of Biological Engineering, Universidade do Minho, Campus de Gualtar, 4710-057 Braga, Portugal;

[4]BCMaterials, Basque Centre for Materials, Applications and Nanostructures, UPV/EHU Science Park, 48940 Leioa, Spain;

[5]Centro Algoritmi, Universidade do Minho, Campus de Azurém, 4800-058 Guimarães, Portugal;

[6]IKERBASQUE, Basque Foundation for Science, 48013 Bilbao, Spain.

*corresponding author: cribeiro@fisica.uminho.pt

Abstract

This work reports on magnetoelectric biomaterials suitable for effective proliferation and differentiation of myoblast in a biomimetic microenvironment providing the electro-mechanical stimuli associated to this tissue in the human body. Magnetoelectric films are obtained by solvent casting through the combination of a piezoelectric polymer, poly(vinylidene fluoride-trifluoro-ethylene), and magnetostrictive particles ($CoFe_2O_4$). The non-poled and poled (with negative and

positive surface charge) magnetoelectric composites are used to investigate their effect on C2C12 myoblast adhesion, proliferation and differentiation. It is demonstrated that the proliferation and differentiation of the cells is enhanced by the application of mechanical and/or electrical stimulation, with higher values of maturation index under mechano-electrical stimuli. These results show that magnetoelectric cell stimulation is a novel and full potential approach for skeletal muscle tissue engineering applications.

Keywords: magnetoelectric biomaterials; muscle tissue engineering; mechano-electrical stimuli; myotubes

Introduction

More than 600 individual skeletal muscles can be found in the human body that enabling to perform a variety of functions, such as executing locomotive tasks, breathing, or moving the eyes, among others [1]. This tissue is the most abundant in human body being one of the components of the musculoskeletal system. Further, it is attached to bones by tendons and produce all the movements of body parts in relation to each other [2].

Skeletal muscle is a highly specialized tissue that consists of striated and elongated multinuclear muscle fibers (known as myofibers) encapsulated within connective tissue sheats [3]. It has the property of plasticity, which mean that when the skeletal muscle is under the influence of physiological changes such as mechanical stress and unloading, the composition of fiber types of skeletal muscle can change [2, 4]. The loss of functional muscle from genetic disease, such as Duchenne muscular dystrophy, traumatic injury or surgical excisions results in a physiologic deficiency that continues to remain without an effective clinical treatment [5].

The replacement and/or regeneration of lost/damaged tissues or organs represent one of the main challenges of the last decades, so in order to address these issues, tissue engineering (TE) has emerged

as a possible solution. In this way, TE represent an alternative and helpful approach for organs/tissues reconstruction/replacing when the conventional pharmaceutical treatments are no more applicable [6]. One of the most important components of the TE multidisciplinary field is the scaffold design that should mimic the naturally exiting extracellular matrix through a complete biomimicking approach, including structural, biochemical and biophysical clues, in order to provide a proper cell growth. In fact, it has been demonstrated that chemical, biological and/or physical signals affect the cell response, enhancing cell target functions such as adhesion, proliferation, migration and differentiation [7]. Among the physical stimuli, it has been shown that mechanical and electrical effects affect biological entities. The cellular responses to mechanical stimuli are mediated by mechanotransduction pathways that can promote tissue development and/or function. Similar to the mechanical stimulation, electrical stimulation influences the survival, proliferation rate, hypertrophy and other properties of muscle cells. *In vitro*, the use of electrical stimulation has been aimed mainly at mimicking the motoneurons action found in their native physiological environment [8].

In the area of muscle TE physical stimuli have been poorly investigated. However, as this tissue reacts to electro-mechanical stimuli during its normal function [8-9], scaffolds that can provide electroactive physical stimuli seems to be a necessary approach. Thus, the application of mechanical and electrical stimulation *in vitro* has shown promise for growing contractile skeletal muscle tissue [10].

In this context, the so-called smart materials and, in particular, smart polymer materials are very interesting for efficient muscle tissue repair strategies. Smart materials are materials that when subjected to an external stimuli, present a significant, reproducible and stable variations of at least one of their properties [11]. In order to provide those physical stimuli (electrical and mechanical) present in the microenvironment of skeletal muscle tissue, electroactive materials, such as piezoelectric polymers, are being increasingly used in the biomedical context [12-14]. These materials develop voltage when a mechanical stress is applied, or vice-versa, promoting adhesion, proliferation and differentiation of myoblast cells. Although muscle itself is not piezoelectric, it is sensitive to dynamic mechanical and electrical solicitations [13, 15], being this dynamic biomimetic approach particularly

relevant as muscle is physiologically subjected to mechano-electrical solicitations related to walking, jumping and running [16-17]. The most representative piezoelectric polymers in this area are poly(vinylidene fluoride), PVDF, and its copolymer due to their biocompatibility, bio stability and high piezoelectric coefficients [11, 14].

Most of the research in the area of muscle TE has been conducted in order to develop scaffolds, mainly varying their morphology in the form of films and fibers as well as by the addition of conductive materials [18]. However, so far, the effect of mechano-electrical stimuli on the myotube differentiation thought polymeric biomaterials that can provide both stimuli simultaneously have not been investigated. As a complement to piezoelectric biomaterials, which will now work under static conditions, for example when the patient is immobilized (for example due to serious health problems), magnetoelectric biomaterials allow to produce magnetically activated mechanical and electrical stimuli. These materials consist on the combination of magnetostrictive particles and piezoelectric materials, the magnetoelectric effect resulting from the mechanical deformation induced by a magnetic field due to the magnetostriction of one of the components, leading to an electrical polarization variation due to the piezoelectric effect of the other phase. Thus, the use of an external magnetic field allows to remotely control tissue stimulation [19] by inducing both mechanical and/or electrical signals to the surrounding tissues [20]; providing an innovative tool for skeletal muscle that has not been evaluated so far.

In this context, this work reports on the development of magneto-active films based on a piezoelectric polymer - poly(vinylidene fluoride-trifluoro-ethylene) (P(VDF-TrFE)) – and magnetostrictive nanoparticles - cobalt ferrite nanoparticles ($CoFe_2O_4$). This composite has been used for biomedical applications The copolymer P(VDF-TrFE) was selected due to its biocompatibility and highest piezoelectric response among polymer and the $CoFe_2O_4$ particles due to the high magnetostrictive response, leading to improved magnetoelectric coupling. For biomedical applications, P(VDF-TrFE) has been selected instead PVDF, as it crystallizes in the ferroelectric phase even when processed from the melt, which is important for the preparation of magnetoelectric composite films [21]. These

composites materials have been evaluated as biomaterials for muscle TE by studying the influence of the mechano-electrical stimuli on myotube differentiation both under static and dynamic conditions.

2-Materials and methods

2.1-Materials

Poly(vinylidene fluoride trifluorethylene) (P(VDF-TrFE)) was acquired from Solvay, N,N-dimethylformamide (DMF), pure grade from Merck and cobalt ferrite nanoparticles ($CoFe_2O_4$, CFO) with 35-55 nm were purchased by Nanoamor.

2.2-Preparation of the magnetoelectric nanocomposites

The films were prepared based on the method presented in [22-23] for similar polymer-based composite compositions.

In order to obtain a good dispersion of the magnetostrictive nanoparticles within the polymer matrix, first, the desired content of CFO nanoparticles (20 wt.%) was added to the DMF and placed in an ultrasound bath (ATU ATM3LCD) during 30 min. Then, citric acid (0.02 $g.mL^{-1}$) was added to the mixture, which was in the ultrasound bath for another 3 h. After this time, P(VDF-TrFE) at a concentration of 20/80 polymer/solvent (w/w) was added to the mixture that was kept under mechanical stirring for 2 h. When the polymer reached complete dissolution, the samples were obtained by solvent casting method, by spreading the solution on clean glass substrate and placing them inside an oven for 10 min at 210 ºC. The films are obtained with ≈ 40 µm of thickness.

Electrical poling of the CFO/P(VDF-TrFE) composites was achieved, after an optimization procedure, by corona discharge inside a home-made chamber (10 kV for 120 min at 120 ºC) and cooling down to room temperature under applied electric field. The piezoelectric response ($d_{33} \approx |8\text{-}10|$ $pC.N^{-1}$) of the poled films was obtained with range d_{33}-meter (model 8000, APC Int Ltd). After

the polarization, average positive charge is obtained in one side of the sample and negative charges on the opposite side. The films used for cell culture are represented in table 1.

Table 1 - Nanocomposites used for cell culture.

Samples	**Polarization**	**$\|d_{33}\|$ ($pC.N^{-1}$)**	**Stimuli given to the cells**	**Denomination**
CFO/P(VDF-TrFE)	None	-----	Mechanical	non-poled
	Positive	9	Mechano-electrical	"poled +"
	Negative	10	Mechano-electrical	"poled –"

2.3-Characterization of the nanocomposites

The morphology of the CFO/P(VDF-TrFE) nanocomposites surface was evaluated by scanning electron microscopy (SEM) with a Hitachi S-4800 device at an acceleration voltage of 10 kV. All the samples were placed in the aluminum pin stubs with electrically conductive carbon adhesive tape.

Tapping mode Atomic Force Microscopy (AFM) images were acquired using an AFM equipment (Nano-Observer CSI). The AFM images were processed using Gwyddion software. The average roughness (Ra) was calculated for each image after three measurements performed in different places of each samples.

Magnetic hysteresis loops were measured at room temperature using a vibrating sample magnetometer (VSM) (Microsense 2.2) from -18500 Oe to 18500 Oe.

Water contact angle (WCA) measurements of the different CFO/P(VDF-TrFE) samples were measured by the static sessile drop method using a Data Physics OCA20 instrument with ultrapure water. The contact angles were measured using the SCA20 software through the water droplets (3 µL) deposited on the sample surface. Each sample was measured at six different locations and the mean contact angle and standard deviation were calculated.

2.3.1 Characterization of the magnetic and electromechanical stimulus

As the magnetoelectric stimulation of the cells on the prepared films is carried out in a bioreactor that applies a varying magnetic field [20], the magnetic characterization of the surface was performed, at the same height of cell culture, in relation to the permanent magnet table, allowing the comparison with the results obtained through the biological analysis with the magnetic stimuli actually produced.

This characterization was performed using a GM08 gaussmeter, with a PT8029 reference Transverse probe, which allows measuring AC and DC fields with maximum amplitude of 3,000 T, using an RS232 connection to record the acquired data.

In order to ensure the correct measurement of the magnetic field, concentric measurements were performed in the centre of the culture wells by displacing the measuring tip along the two axes, which is coupled to a graduated X-Y table.

To better understand the field format, based on the characteristics of the bioreactor magnets and the values recorded in the measurement, a finite element modelling was performed using the ANSYS Maxwell software, obtaining a three-dimensional analysis of the generated magnetic fields. After the magnetic component was analysed, the magnetically induce deformation of the samples by the magneto-mechanical transduction was also characterized by attaching a strain gauge (L2A-06-062LW-120) to the sample using a LOCTITE Hysol® 3425 two-component araldite glue. The sensor variation measurement is based on a setup developed for this purpose, given the need to obtain a relatively high sampling rate, taking into account the bioreactor operating frequency (200 samples per second), and high resolution, due to the low deformation of the sample.

Resistance variation of the strain gauge was obtained by measuring the voltage at the sensor terminals using a 24 bit sigma delta ADC with reference LTC2440 controlled by Evaluation Board DC590B, connected via USB to the computer. DC590. In order to measure the resistance variation through voltage variation, a precision constant current was applied using Keithley 2400 Source/Meter, where a 1 mA reference current was applied.

Finally, the characterization of the electrical response of the biomaterial –magnetoelectric stimulation- when positioned on the wells of culture plate was performed using an external setup to

the bioreactors-biomaterial system. The wide range d33-meter (model 8000, APC Int. Ltd., Mackeyville, PA, USA) was used to obtain the piezoelectric response (d_{33}) of the samples, and the magnetoeletric effect was characterized by measuring the transverse ME voltage coefficient (α33) and longitudinal ME coefficient (α31) using the dynamic lock-in amplifier method. The samples were placed in the center of a ME characterization system composed by two sets of concentric Helmholtz coils. A pair of coils was used to generate an AC field with amplitude of 1 Oe, at the resonant frequency of the sample, simulating the AC response applied by the bioreactors. The second set of Helmholtz's coils allows varying the DC magnetic field applied to the sample from 0 to 0.5 T, controlled by a current power source. The voltage generated in the direction of sample thickness was measured using a digital Lock-in amplifier (Stanford Research SR530). ME stress coefficients were calculated from the measured strain using equation 1.

$$\alpha_{33} = \frac{\Delta V}{H_{AC} * t} \qquad (1)$$

where ΔV is the measured output voltage, H_{AC} is the amplitude of the AC magnetic field, and *t* is the thickness of the piezoelectric layer.

The characterization of the electrical response in the mechanical bioreactor was performed by measuring the piezoelectric response of the sample under mechanical stimulation. Conductive electrodes were printed on the surface of the sample by screen printing, the sample was connected to a 16 bits high resolution oscilloscope (PicoScope 4262) and the electrical response as a function of frequency recorded.

2.3-Cell culture assays

2.3.1-Samples sterilization

For the *in vitro* assays, circular CFO/P(VDF-TrFE) films (non-poled, “poled +” and “poled –”) were cut with 13 mm of diameter. These samples were sterilized by multiple immersions into 70% ethanol

for 30 min each and washed 5 times in a phosphate buffered saline (PBS 1x) solution for 5 min each to remove any residual solvent. Subsequently, the samples were exposed to ultraviolet (UV) light for 2 h (1 h each side). Then, the samples were placed in 24-well cell culture plates.

2.3.2-Cell culture

C2C12 cells were grown in 75 cm^2 cell-culture flask and cultured in basal medium (BM), consisting of Dulbecco's Modified Eagle's Medium (DMEM, *Gibco*) containing 4.5 $g.L^{-1}$ supplemented with 10% Fetal Bovine Serum (FBS, *Biochrom*) and 1% Penicillin-Streptomycin (P/S, *Biochrom*). The flask was incubated at 37 ºC in a humidified air containing 5% CO_2 atmosphere. The culture medium was changed every two days and when the cells reached 60-70% confluence, they were trypsinized with 0.05% trypsin-EDTA.

2.3.3-Adhesion assays

For cell adhesion tests, C2C12 cells were seeded at a cell density of 4 000 $cells.cm^2$ with a drop of 100 µL in 24-well plates and allowed to adhere in the CFO/P(VDF-TrFE) nanocomposites for 45 min at 37 ºC, and then 400 µL of DMEM was added to each well (drop method). After 24 h of culture in BM, C2C12 cells were subjected to immunofluorescence staining in order to analyze the presence of focal adhesions. At this time, the medium of each well was removed and the cells were washed with PBS 1x and fixed in 4% formaldehyde for 10 min at 37 ºC. The nucleus, actin and vinculin were stained by 4',6-diamidino-2-phenylindole (DAPI, *Sigma-Aldrich*), Tetramethylrhodamine B isothiocyanate (TRITC, *Sigma-Aldrich*) and anti-vinculin−FITC antibody (*Sigma-Aldrich*), respectively. After this, the samples were again washed with PBS 1x and then incubated with anti-vinculin−FITC antibody (1:50 in PBS 1x) in the dark at room temperature for 1 h. The cells were subsequently counterstained with TRITC (1:200) and DAPI (1 $\mu g.mL^{-1}$) at room temperature in the dark for 30 and 5 min, respectively. At the end, the samples were rinsed in PBS 1x and after with

distilled water, and finally mounted on slides. The samples were visualized using a fluorescence microscope (*Olympus Bx51*) with the appropriate filter sets.

2.3.4-Proliferation and differentiation cell culture assays

C2C12 cells were seeded on the different CFO/P(VDF-TrFE) nanocomposite films at a density of 7 500 and 40 000 cells.cm^2 for proliferation and differentiation tests, respectively (figure 1). Similarly, to the cell adhesion assays, the drop method was used for the proliferation and differentiation assays. For cell proliferation studies, two plates at these conditions were incubated with BM at 37 ºC in a saturated humidity atmosphere containing 95% air and 5% CO_2 for 24 h to allow cell adhesion. After this time, one plate was maintained at the same conditions (static culture – cell culture without any applied stimuli) and the other was transferred onto a home-made bioreactor [20] system (dynamic culture – cell culture under magnetic stimulation for magneto-mechanical and magneto-electric response) up to 3 days.

For the differentiation experiments, the samples were placed in 24-well plates (three plates) and incubated in BM, as previously described, until reached 90% confluence. Thereafter, in order to induce myotube formation, the BM of half of the samples was changed to differentiation medium (DM). The DM was composed of DMEM supplemented with 2% FBS and 1% P/S. As for the proliferation assay, one plate was maintained at the same conditions (static culture), other was transferred onto the magnetic bioreactor (dynamic culture) and the last one to a mechanical bioreactor (dynamic culture) up to 8 days. In all conditions, the medium was renovated daily.

For the dynamic culture (figure 1), the samples placed on the magnetic bioreactor were subjected to the following cycle, as presented in [20]: an active time of 16 h under magnetic stimulus (divided into 5 min of active time and 25 min of repose time) followed by a non-active time of 8 h (no magnetic stimulation). The dynamic culture was performed under magnetic stimulation at a frequency of 0.3 Hz and the 20 mm displacement of permanent magnets below the culture wells.

In parallel, for differentiation tests, another home-made bioreactor system was used with mechanical stimulation (see [24-25]) by placing the culture plate on a vertical vibration module at a frequency of 1 Hz with amplitude of approximately 1 mm. The following cycle has an active time of 16 h under mechanical stimulus followed by a non-active time of 8 h (no mechanical stimulation), in order to mimic the human body mechanical stimulation along a day, such as in the magnetic bioreactor (figure 1).

In each study, 3 replicates were used for each condition.

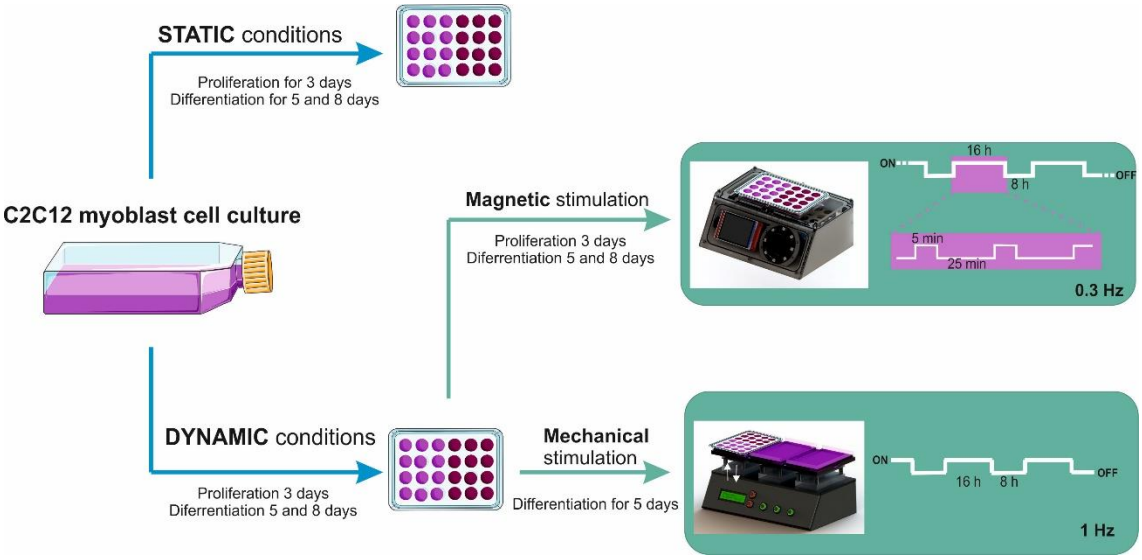


Figure 1 - Schematic representation of the cell culture assays using static and dynamic (magnetic and mechanical stimulation) conditions and parameters applied by each bioreactor.

Both bioreactors allow to provide a mechano-electrical stimulation to the cells, but with different intensities, as it will be discussed later.

2.3.4.1-Cell viability

For the proliferation assays, the evaluation of the cell viability of C2C12 myoblast on the different CFO/P(VDF-TrFE) films under static and dynamic conditions was analyzed by the (3-(4,5-dimethylthiazol-2-yl)-5-(3-carboxymethoxyphenyl)-2-(4-sulfophenyl)-2H-tetrazolium) (MTS) assay. The MTS assay was carried out after 1 and 3 days and at these time points, the cell/films were transferred to new wells and fresh medium containing MTS solution (1:5 proportion of DMEM medium) was added. The plate was incubated at 37 °C for 2 h and, then, the absorbance was measured

at 490 nm with a microplate reader (Biotech Synergy HT). The cell proliferation values were determined regarding the cells adhered on the material after 24 h adhesion, just before placing them in contact with the bioreactor (equation 2). Experimental data were obtained from four replicates of each sample of three independent experiments and expressed as mean ± standard deviation (SD).

$$Cell\ proliferation\ (\%) = \frac{Abs_{490nm}\ sample}{Abs_{490nm}\ sample\ after\ 24h\ adhesion}\ x\ 100 \qquad (2)$$

2.3.4.2-Immunofluorescence staining

For proliferation and differentiation studies, immunofluorescence tests were also performed to analyze the cytoskeleton morphology of the cells, and also verifying the cell viability and the presence of myosin heavy chain (MC), respectively.

For proliferation tests under static and dynamic (magnetic stimulation) conditions, after 3 days, the same point used for MTS evaluation, some samples were subjected to immunofluorescence staining. For that, the medium of each well was removed, the samples were washed with PBS 1x and fixed with 4% formaldehyde for 10 min at 37 ºC in a 5 % CO_2 incubator. After fixation, the samples were washed with PBS 1× (three times) and incubated for 45 min at room temperature in 0.1 µg mL^{-1} of green phalloidin (*Sigma-Aldrich*). Then, the samples were incubated for 5 min with 1 µg mL^{-1} of DAPI. Afterwards, the samples were washed again with PBS 1× (three times) and one time with distillate water. Finally, the samples were visualized with fluorescence microscopy (Olympus BX51 Microscope).

For differentiation tests under static and dynamic (magnetic and mechanical stimulation) conditions, after 5 and 8 days of differentiation, the medium of each well was removed and the cells were washed with PBS 1x and fixed in 70% ethanol-37% formaldehyde-glacial acetic acid (20:2:1) solution for 10 min at 37 ºC and then blocked with a blocking solution (5% goat serum and 0.3% triton X-100 in PBS 1x) for 1 h at room temperature. After this, the samples were incubated with monoclonal mouse IgG_{2B} Clone MF20 antibody (R&D Systems, Catalog number MAB4470) at 1:50 in 5% goat serum

in PBS 1x at room temperature for 1 h, washed in 0.5% PBS-Tween 20 and then labelled with anti-mouse IgG-NL557 secondary antibody (R&D Systems) diluted 1:200, also in 5% donkey serum in PBS 1x at room temperature and in the dark for 1 h. The cells were subsequently counterstained with DAPI for 5 min at room temperature in the dark, rinsed in 0.5% PBS-Tween 20 and then with distilled water. The samples were carefully removed from the wells, mounted on slides with the cells facing towards the microscope slide and visualized using a fluorescence microscope (Olympus BX51) with the appropriate filter sets for the used label.

2.3.4.3-Calculation of fusion and maturation index per area

The fusion index was calculated as the ratio of the nuclei number in myotube with two or more nuclei versus the total number of nuclei. The maturation index was defined as myotubes having five or more nuclei. Myotube number per area was calculated by dividing the number of myotubes in each pattern by the respective area of the pattern and after converted to an area of 1 mm^2. Length, width and the ratio between them was also calculated. All the tests were performed using data obtained with the ImageJ software. Experiments were carried out on three samples for each condition and by analyzing ten images for each sample, for each of the two independent experiments. The graphs were designed in OriginPro 8.5, and Photoshop CS5 was used to assembly the figures for publication. Data are presented as mean ± standard error of mean (s.e.m.) from triplicates of two independent experiments.

2.3.4.4-Quantification of creatine kinase activity

For cell differentiation assays, creatine kinase activity (CK) was also quantified. For that, the cells present in the samples were rinsed with PBS 1x and collected with a cell scraper. After that, the cells were homogenized in an appropriate volume of cold 50 mM potassium phosphate (pH 7.5) buffer and centrifuged at 10 000 ×*g* for 15 min at 2-8 ^{0}C. After the centrifugation, the supernatant was removed and used for the assay. Creatine kinase activity of the samples was determined using a commercially

kit (*Sigma-Aldrich*). The kit is based on enzyme coupled reactions in which creatine phosphate and ADP is converted to creatine and ATP by creatine kinase. The generated ATP is used to phosphorylate glucose by hexokinase to generate glucose-6-phosphate, which is then oxidized by NADP in the presence of glucose-6-phosphate dehydrogenase. The produced NADPH, measured at 340 nm, is proportionate to the CK activity in the sample. Data are presented as mean ± s.e.m. from triplicates of two independent experiments.

2.3.5-Statistical Analysis

All quantitative data were analyzed using GraphPad Prism (v6.00, La Jolla, CA, USA). The results were analyzed statistically using the two-way ANOVA followed by Tukey's test. Differences were considered to be statistically significant when p-value < 0.05.

3 - Results and Discussion

3.1- Characterization of CFO/P(VDF-TrFE) nanocomposites

When cells adhere to the surface of a scaffold, a sequence of physico-chemical reactions will occur, influencing cell fate. The cell attachment is a complex process, affected by numerous aspects, such as material surface properties. Thus, relevant properties of the CFO/P(VDF-TrFE) films surface were investigated.

The CFO/P(VDF-TrFE) composites films with the same amount of CFO nanoparticles (20 wt.%) and different polarization state were analyzed by SEM (figure 2a, 2b and 2c). It is observed random fibril-like microstructure (see inset of figure 2a) as a result the characteristic growth of the co-polymer, which crystallization kinetics is hindered by the presence of the CFO nanoparticles, acting as nucleation agents for crystallization [26]. It is also observed that the distribution of the magnetostrictive nanoparticles within the P(VDF-TrFE) polymer matrix is uniform without large agglomerations and that the films are non-porous. Those characteristics are independent of the poling state.

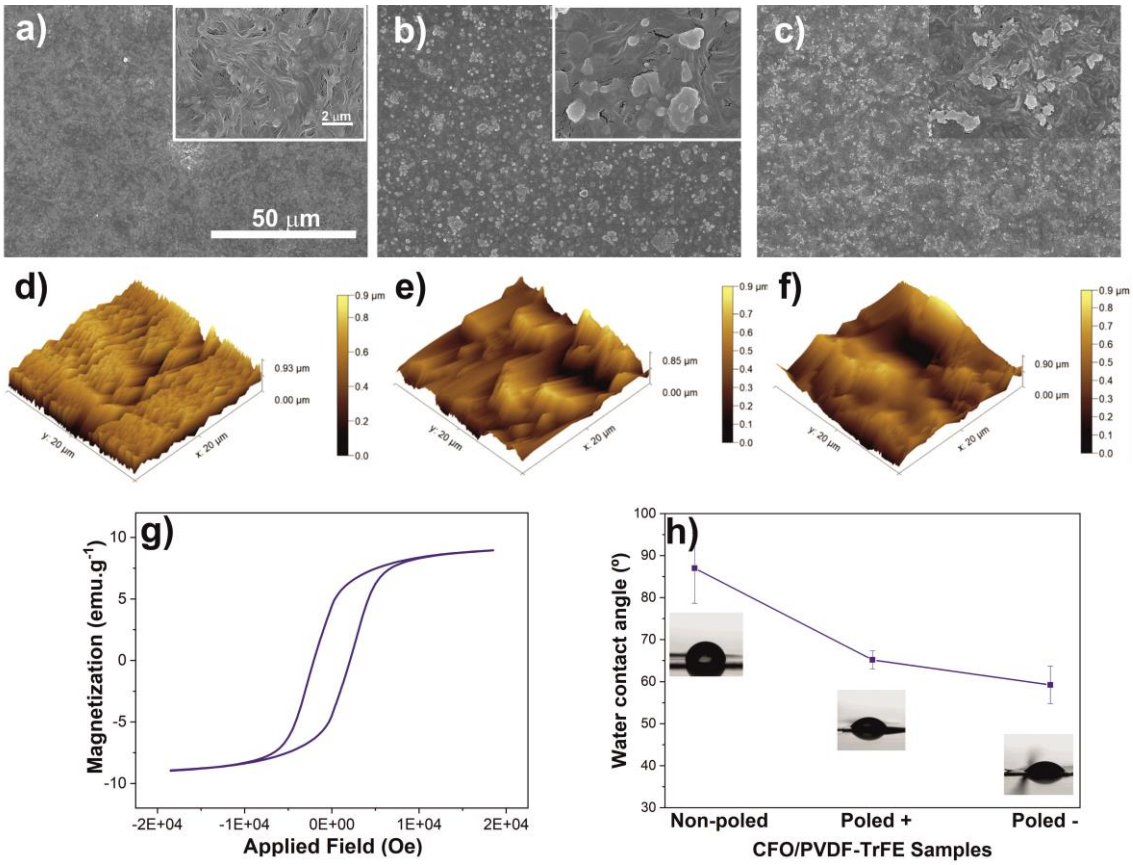


Figure 2 - Surface morphology obtained by scanning electron microscopy of the CFO/P(VDF-TrFE) nanocomposite films: (a) non-poled, (b) "poled +" and (c) "poled -". The scale bar is 50 µm for all the images and 2 µm for the inset images. The corresponding AFM (20 × 20 µm) results are presented in figures, d), e), f), for CFO/P(VDF-TrFE) non-poled, "poled +" and "poled -" materials, respectively. (g) Room temperature hysteresis loops for CFO/P(VDF-TrFE) films. (h) Water contact angle measurement for CFO/P(VDF-TrFE) films with and without polarization (mean ± SD).

The AFM images of the CFO/P(VDF-TrFE) samples with different polarization are displayed in figure 2, maintaining the same scale and scan size for comparison. The inclusion of CFO nanoparticles in the P(VDF-TrFE) matrix lead to an average roughness of ≈ 83 ± 19 nm for the CFO/P(VDF-TrFE) non-poled films. When these samples are subjected to the polarization procedure, a slight decrease in the roughness occurs, with no significant differences between both polarizations states: ≈ 78 ± 21 nm for the negative and ≈ 75 ± 20 nm for the positive one. This decrease can be associated with the fact that the polarization induces more ordered structures [27] and with the homogenization effect of the plasma in the polymer surface [28].

The quantification of the magnetic nanoparticle content within the composites was assessed by VSM technique. The hysteresis curves (figure 2g) reveal a typical ferromagnetic behavior for the nanocomposites with CFO nanoparticles [29], characterized by magnetization curves in which the magnetization increases with increasing magnetic field until saturation, reaching a maximum saturation of 8.9 $emu.g^{-1}$ at approximately 20 000 Oe.

Once the surface wettability (hydrophobocity/hydrophilicity) is an important parameter that affects cell-biomaterial interaction and, therefore, cell behavior, the wettability of the different samples was assessed through sessile drop technique (figure 2h). All samples show contact angles below 90º, presenting a hydrophilic behavior, which is agreement concordance with the literature [30]. The introduction of CFO nanoparticles (≈ 87 ± 8º for non-poled CFO/P(VDF-TrFE) films slightly increases the contact angle comparatively to the P(VDF-TrFE) film without CFO (≈ 78 ± 5º) [28], further, the polarization process strongly affects the wettability of the samples, leading to a decrease in the contact angle values: with positive polarization, the value decreases to ≈ 65 ± 2º, whereas with negative polarization, the value decreases to ≈ 59 ± 4º. These results are in agreement with previous studies were it was demonstrated that corona treatment produce an increase in the surface wettability [31], based on the alignment of the dipolar moments and, therefore, the net surface charge (positive or negative) in the poled samples [32].

There are numerous approaches in an attempt to promote cell proliferation and cell differentiation, approaches that recently include the incorporation of responsive materials used as scaffolds with electrical, magnetic and/or electromechanical properties, associated with the use of new generations of bioreactors [11], which allow control and stimulation of these new materials. In this way, it is important to characterize the stimuli that actually reach to the material where the cells are in contact. In this work, the materials used are subjected to a variable magnetic field, produced by a home-made magnetic bioreactor [20], where the emergence of a magneto-mechanical oscillation in the

magnetostrictive nanoparticles will produce the electrical response in the piezoelectric polymer, leading to a magnetically activated electroactive microenvironment.

In this way, an experimental setup was developed to measure the quantities effectively applied to the material surface and transmitted to the cells. Given the characteristics of the material used, the first major transduction that occurs corresponds to a magnetic stimulus that translates into an applied mechanical stimulus to the cells. Therefore, in a first phase, the magnetic field dispersion to which the magnetoelectric film is subjected was measured. It was found that the films are subjected to a magnetic field that varies between 0.22 T and -0.22 T, according to the position of the magnets relative to the material. Thus, a finite element simulation of the field-to-surface dispersion was performed, based on the magnetic bioreactor characteristics, and the fields measured by a gaussmeter (figure 3).

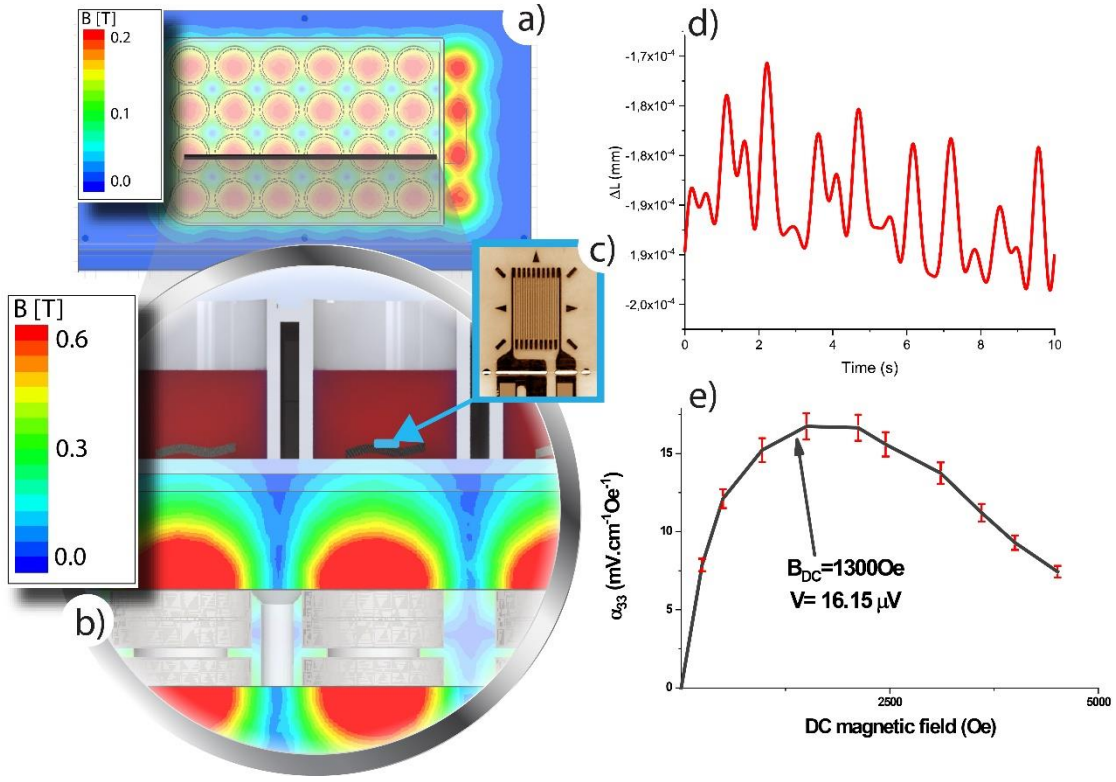


Figure 3 - a) Result of the simulation process, along the material surface; b) cross-section image of the field created along the distance between the permanent magnet and the material surface; c) detail of the strain gauge sensor for the measurement of the materials deformation; d) result of the strain measurement, obtained from the measurement of the

sensor resistance variation; e) Magnetoelectric response of CFO/P(VDF-TrFE) for a DC field from 0 to 5000 Oe at a constant H_{ac} of 1 Oe.

Figure 3 shows the magnetic field variations, being the magnetic field approximately zero in the central regions between the magnets. Further, there are slightly larger fields in the peripheries of the culture plated when compared to the central region.

After the analysis of the field applied to the magnetoelectric films, the mechanical strain was measured with a strain gauge sensor (L2A-06-062LW-120, Micro-Measurements) coupled to the film (figure 3c). Once the bioreactor is placed into operation, the resistance variation of the strain gauge was obtained, as shown in figure 3b. It is important to note that the sensor was placed at the centre of the well, concentric with the bioreactor excitation magnet, where a displacement cycle was applied allowing the movement of the table until the sensor was concentric with the neighbor magnet, corresponding to a total displacement of 20 mm at a frequency of 0.3 Hz leading to an approximately sinusoidal magnetic excitation with amplitude of approximately 0.22 T in each point. Once the voltage variation at the sensor terminals was collected, the corresponding conversion was carried out to resistance variation, taking into account the reference current through the application of Ohm's law. In order to obtain the mechanical variation of the film, the conversion of the resistance to the deformation variation is performed taking into consideration the gauge factor of the sensor, 2.155, and its length along the measurement axis, 1.52 mm. Thus, the dimensional variation of the sample over the various magnetic excitation cycles is obtained as represented in figure 3d, which shows the uniformity of the response over the various magnetic cycles. In this way, it can be concluded that the magnetoelectric films present a variation of approximately 0.02 μm, which corresponds to a variation of 0.013 $\mu m.mm^{-2}$, since the deformation along the transversal and longitudinal axis is the same, for the already mentioned variation of magnetic field.

Finally, magnetoelectric characterization (figure 3e) shows that the samples present a maximum electrical response for an applied DC field of 1500 Oe. However, the DC component of the magnetic field produced by the home-made magnetic bioreactor is around 2200 Oe (0.22T), being at the

biomaterial level around 1300 Oe, which correspond to a magnetoelectric response of the material of 16.15 μV.

Relatively to the electrical response obtained when the sample is placed on the mechanical bioreactor, a response of 64 μV was measured at a mechanical vibration frequency of 1 Hz.

3.2 - Cell Culture Results

The surface properties of the biomaterials, namely the wettability, roughness and surface charge have demonstrated to be the three most important factors affecting cell adhesion [33]. Regarding the wettability, it is expect that a decrease of WCA lead to an increase of cell adhesion [34]. Relatively to the roughness, it has been demonstrated that the sub-microenvironment variations associated to the microscale roughness lead to different response depending on cell type [35]. Additionally, it has been demonstrated that the surface charge can influence the cell behavior, where the negative or positive charges can enhance different types of cells, being an essential factor determining the regulation of cell response [36]. Moreover, it has been proven that charged surfaces and piezoelectric materials enhance skeletal muscle tissue regeneration [12-13]. However, the influence of the mechano- and/or mechano-electrical stimuli on muscle proliferation and differentiation has not been studied yet. The selected scaffolds were in the form of compact films, in order to study the effects of the different stimuli without further morphological influences, such as porous or fibrilar structures. So, three different samples were used to prove the suitability of the magnetoelectric materials as a new magnetically activated electroactive microenvironment approach for skeletal muscle tissue regeneration [20]. In the present case, the non-poled samples present higher WCA than the poled ones, with no significant differences between the samples with different surface charge, as verified above. In this way, for the CFO/P(VDF-TrFE) poled samples, the major differences between them is just the surface charge being positive or negative. Taking this into account, the effects of the magnetoelectric films with different surface charges on myoblast cell adhesion, proliferation and differentiation were first investigated.

3.2.1 - C2C12 cell adhesion and proliferation on CFO/P(VDF-TrFE) composites

The influence of the surface charge of the CFO/P(VDF-TrFE) films on the adhesion of C2C12 myoblast were first studied after 24 h of cell culture under static conditions. Figure 4 shows the fluorescent images in which the cells were stained for nucleus (blue), F-actin (red) and vinculin (green).

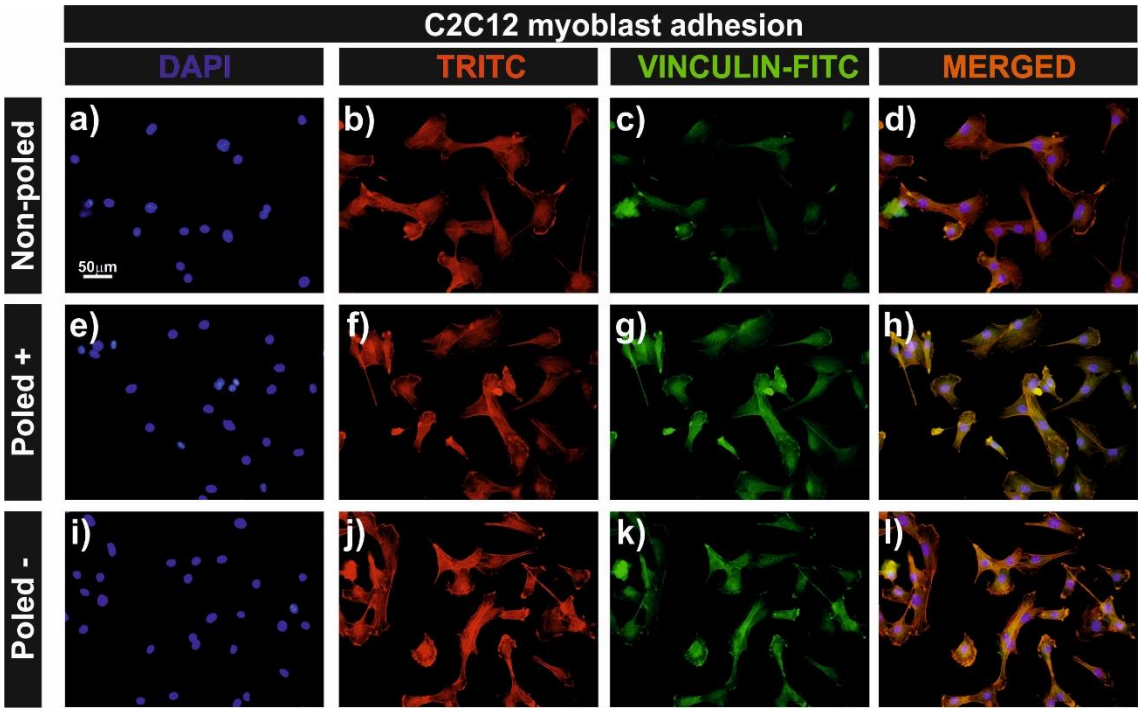


Figure 4 - C2C12 myoblast cells cultured on the surface of CFO/P(VDF-TrFE) nanocomposite films (non-poled, "poled +" and "poled –") after 24 h of cell adhesion. Fluorescence images of DAPI stained cell nuclei (blue) in a), e), and i); F-actin expression (red) in b), f) and j); vinculin staining (green) in c), g) and k); and overlay in d), h) and l). The scale bar (50 µm) is valid for all the fluorescent images.

The investigation of the cell-matrix contacts in the cells cultured on CFO/P(VDF-TrFE) nanocomposite films with different charges is a relevant issue to understand the influence of substrate polarization on focal adhesion characteristics. It has been reported that cell adhesion to a substrate is a key factor determining the function of adhesion receptors in the recruitment of proteins that link the

adhesion receptor to the actin cytoskeleton [37]. In this sense, figure 4 shows the presence of vinculin, a cytoplasmic actin-binding protein, throughout all the cytoplasm of C2C12 cell in all the samples, independently of the sample surface charge and properties. Relatively to the intensity, it appears to be higher on poled samples than on the non-poled one, and between the different surface charges, it seems to be slightly higher on the positive ones. Analyzing the morphology of C2C12 cells, it is observed that C2C12 cells cultured on poled (negative and positive) CFO/P(VDF-TrFE) surfaces demonstrate a greater spreading morphology with those on the non-poled CFO/P(VDF-TrFE). The same behavior was observed in the C2C12 myoblast cells cultured on piezoelectric β-PVDF film [38].

As previously indicated, muscle tissue reacts to an electro-mechanical environment and for that, piezoelectric polymers can deliver a mechanical (with non-poled samples) or mechano-electrical signal to the cells (with poled samples) in order to mimic signals and effects present in living tissue. It has been in fact proven that surface charge of β-PVDF poled samples have impact on C2C12 myoblast adhesion, proliferation [12] and differentiation [13]. However, the effect of mechanical and/or electrical stimuli on the cell behavior through the use of electroactive biomaterials has not been studied yet. In order to address those issues, magnetoelectric samples, that consist on the combination of magnetostrictive (CFO) and piezoelectric (P(VDF-TrFE)) materials are proposed. These materials allow to investigate the three kind of effects on the proliferation and differentiation of C2C12 myoblast cells: 1) at static conditions, the potential of these films and the influence of the surface charge; 2) at dynamic conditions, with the non-poled samples, the mechanical stimulation and 3) at dynamic conditions, with the poled samples, the mechano-electrical stimulation (figure 5).

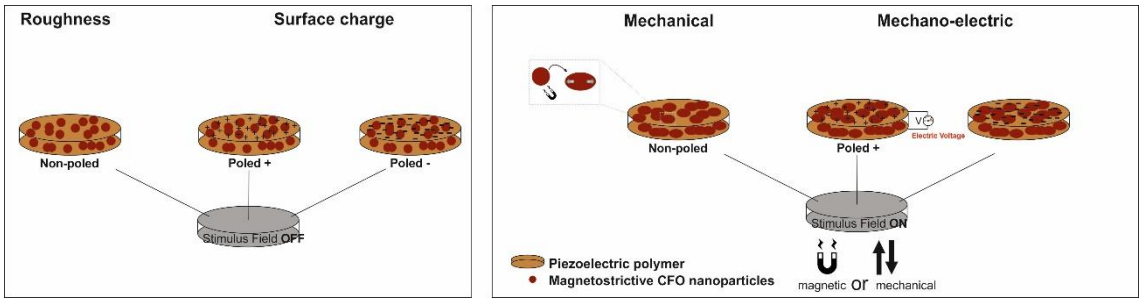


Figure 5 - Representative images of the stimuli provided to the cells by the different samples under different conditions.

The morphology and proliferation of C2C12 myoblasts on the different samples (non-poled, "poled +" and "poled –") were analyzed up to 3 days of cell culture under static and dynamic conditions with immunocytochemistry and MTS assay, respectively (figure 6).

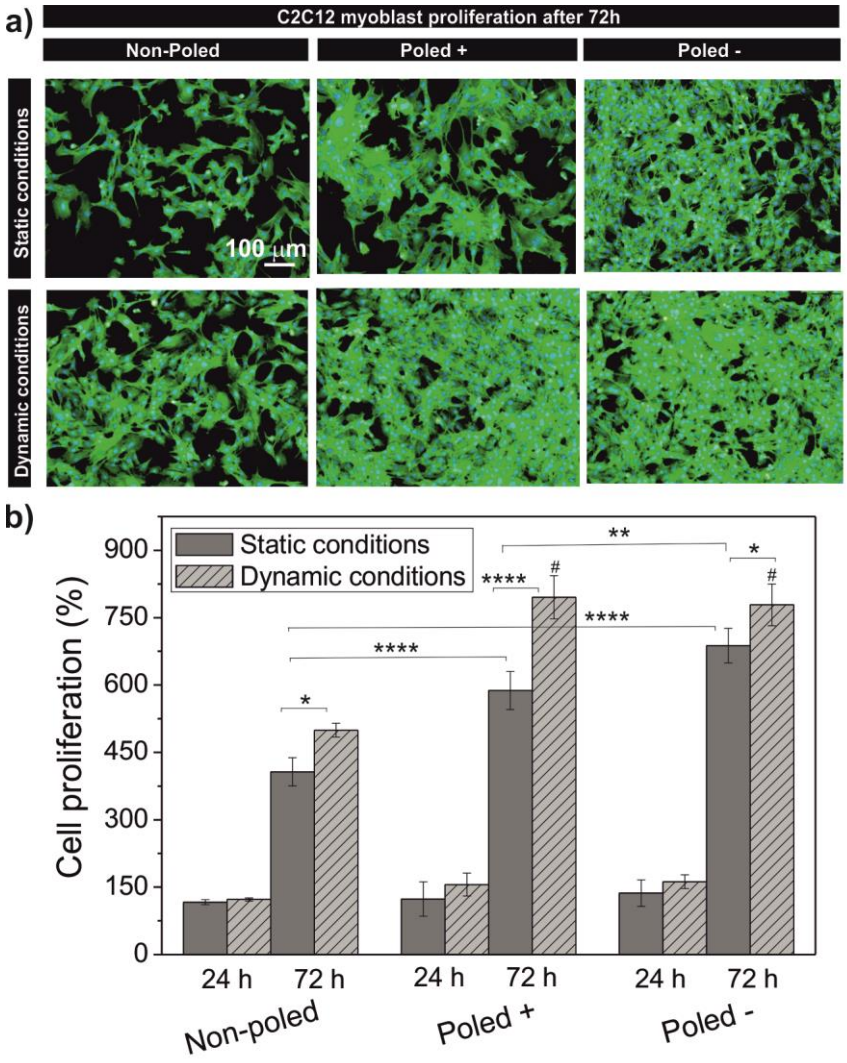


Figure 6 - a) Representative immunofluorescence images (nucleus stained with DAPI - blue and cytoskeleton stained with FITC - green). Scale bar (100 µm) is valid for all images. b) Cell proliferation of C2C12 myoblast culture up to 72 h on CFO/P(VDF-TrFE samples (non-poled, "poled +" and "poled -") under static and dynamic conditions. The cell proliferation values were determined regarding the cells adhered on the material after 24 h adhesion, just before placed in contact with the bioreactor. The results are expressed as the mean ± SD of three independent assays. *$p \leq 0.05$, **$p \leq 0.01$, ****$p \leq 0.0001$ and #$p \leq 0.0001$ *vs* non-poled after 72 h at dynamic conditions.

Figure 6a shows that cell proliferation increases in all samples under static and dynamic conditions from 24 h to 72 h, which is in agreement with the obtained values for cell proliferation (Figure 6b). Under static conditions, and after 24 h of cell culture, the cell proliferation on all CFO/P(VDF-TrFE) materials are similar, with a little difference between the non-poled samples and poled ones. After 72 h, as expected, all samples demonstrated an increase of cell proliferation, with the lower value for the non-poled samples (≈ 405%) and the higher for the "poled –" CFO/P(VDF-TrFE) films (≈ 685%). This behavior is in agreement with a previous studies where was stated that negative surface charges promote higher proliferation rates of C2C12 myoblast cells [12].

Under dynamic conditions (figure 1), the influence of the mechanical and/or electrical stimulation on cell proliferation was studied, showing that both stimulations improve cell proliferation, being significantly higher (figure 6b) with the mechano-electrical stimuli (with poled samples, ≈ 780%), being no significant differences between both polarizations, confirming the myoblast sensitivity to the mechano-electric stimuli.

3.2.3- C2C12 cell differentiation on the CFO/P(VDF-TrFE) samples

During differentiation of C2C12 cells, myoblasts undergo remodeling to form mature myotubes with increased expression of muscle specific genes [4]. Final differentiation into contractile units is concomitant with the expression of sarcomeric proteins such as skeletal muscle myosin heavy chain (MHC). The expression of MHC isoforms is often a measure of *in vitro* myotube differentiation and efficiency [39]. In this study, C2C12 myoblasts were grown on the materials in the presence of two different culture media, basal medium, in order to evaluate just the physical stimuli, and differentiation medium, used to assess the effect of the biochemical stimulus and two different conditions of culture, static and dynamic. These parameters were selected to access the influence of surface charge and mechano-electric stimuli in the expression of the myogenic differentiation marker MHC. Figure 7 shows the fluorescent images of C2C12 myoblasts cultured on the different

CFO/P(VDF-TrFE) films surfaces, as well some relevant properties of the formed myotubes formed, including fusion and maturation index, length, aspect ratio between length and width and the number of myotubes per 1 mm^2.

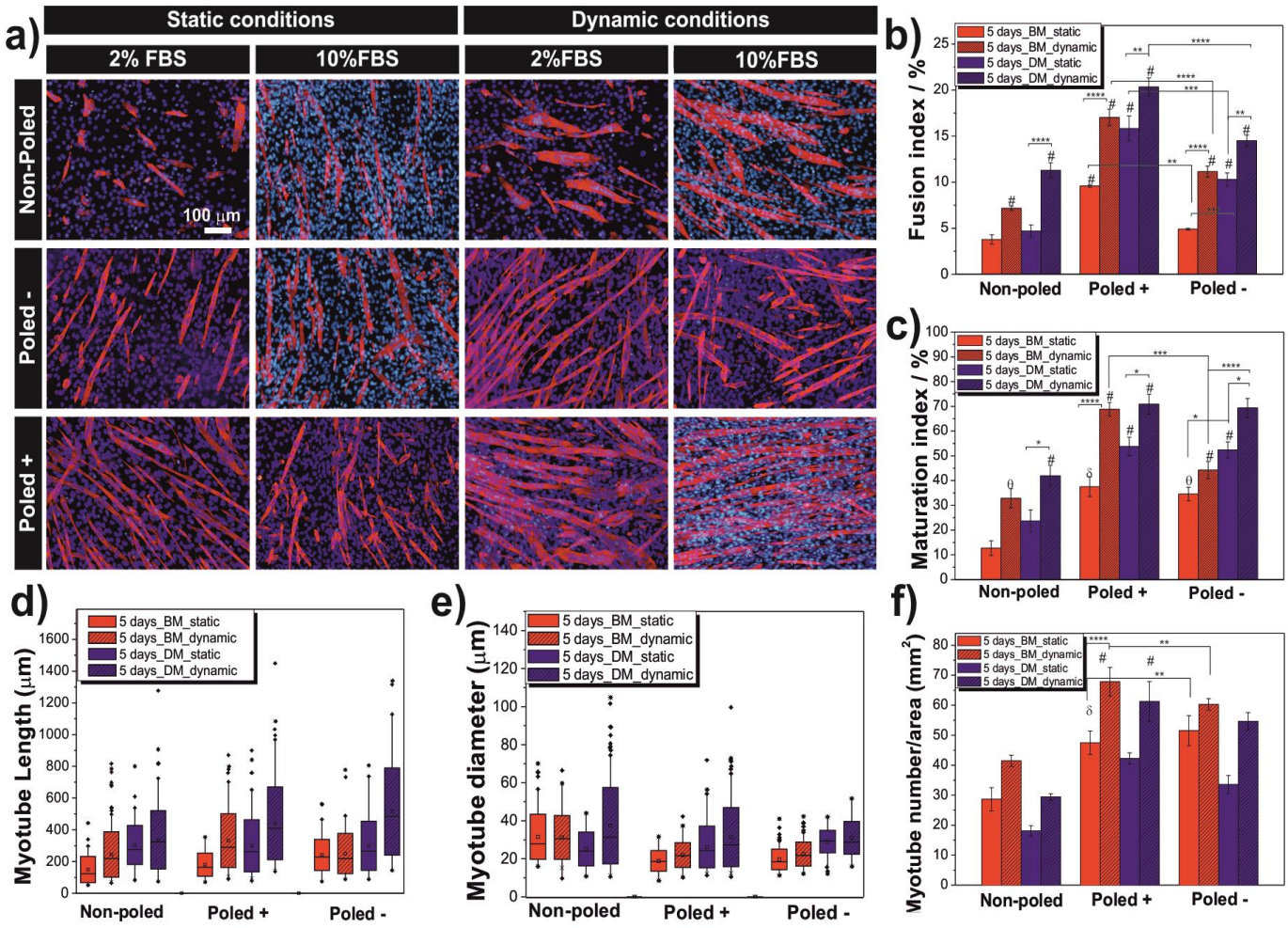


Figure 7 - (a) Immunofluorescent staining of myosin heavy chain after 5 days of C2C12 cells differentiation on the different samples. Row 1 shows the C2C12 cells present on non-poled, row 2 shows them on "poled +" and row 3 shows the cells on "poled -" CFO/P(VDF-TrFE) samples. The columns 1 and 2 show the cells under static condition with DM and BM, respectively; columns 3 and 4 show them under dynamic conditions (magnetic stimulation) with DM and BM, respectively. Quantitative analysis on (b) fusion index, (c) maturation index, (d) myotube length and (e) diameter of the obtained myotubes and (f) myotube number. Data are expressed as the mean ± s.e.m. $^{*}p \leq 0.05$, $^{**}p \leq 0.01$, $^{***}p \leq 0.001$, $^{****}p \leq 0.0001$; *and* $^{\delta}p \leq 0.01$ *vs* non-poled with BM and static conditions, $^{\theta}p \leq 0.001$ *vs* non-poled with BM and static conditions and $^{\#}p \leq 0.0001$ *vs* non-poled with BM and static conditions.

Figure 7a shows that all the magnetoelectric materials with and without surface charge promote myogenic differentiation of C2C12 myoblast that can be confirmed by the presence of MHC in all the samples after 5 days of cell culture in all the conditions. Regarding the fusion index (figure 7b) at static conditions, with BM, the sample "poled +" show higher values comparatively to the other samples that shows similar values. When the medium was changed to DM, significative differences were observed in both poled samples. Also, it is possible to verify significant differences between the polarization surface charges, with higher values for the positively charged samples. Previous studies show related results, proving that electrically poled β-PVDF samples promote higher fusion index values [13], with also higher values for the positive ones. This fact indicates that positively charged samples improves C2C12 myoblast differentiation.

After analyzing the myogenic fusion index, i.e. the number of fused cells per total cell number, it is also important to evaluate the maturity of the formed myotubes.

Relatively to the maturation index (figure 7c) at static conditions, it is verified with BM that poled samples present significant higher values compared to the non-poled ones, but with no significant difference between the polarization types. Changing the medium to DM, the same behavior as the one observed in the fusion index was observed: all samples present higher values with DM but with no significant difference for the non-poled samples and significant difference for the poled ones. However, comparing the poled samples, contrarily to the fusion index, no significant differences were observed among them.

The differentiation assays on the same scaffolds using the drop method (figure 1) under dynamic conditions were performed at the same time. It is observed (figure 7b and 7c) that for all samples with and without DM under dynamic conditions, the values of fusion and maturation index were higher than under static condition. After 5 days of differentiation it is evident, for cell culture in both media, that the fusion index was more significative in charged samples, in particular in “poled +” with DM (≈ 20%). Although significant differences between the polarizations on fusion index values were

observed, similar maturation values were verified for "poled +" and "poled –" with DM (≈ 71 and 69% respectively). The non-poled samples showed ≈ 11 and 42% for fusion and maturation index, respectively, demonstrating that mechanical and mechano-electrical stimuli promote C2C12 myoblast differentiation.

In order to assess the myotube formation, myotube length (figure 7d), diameters (figure 7e) and numbers/area (figure 7f) were evaluated for cell culture with the two media (BM and DM), under static and dynamic conditions. It is verified that non-poled samples lead to higher myotubes diameters and that the poled samples lead to higher myotubes length. Relatively to the myotube number per area, it is verified that the dynamic conditions improve the number of myotubes, with higher values for the poled samples, which is in agreement with the obtained results of fusion and maturation index.

After examination of the myogenic differentiation on CFO/P(VDF-TrFE) samples by the presence of MHC, the major structural protein in myotubes, another muscle-specific structural gene, muscle creatine kinase was evaluated during the differentiation phase. Creatine kinase is a relevant muscle-specific gene in muscle fiber-type maturation of the myotubes. Figure 8 shows the creatine kinase values obtained for C2C12 myoblast cells cultured on CFO/P(VDF-TrFE) films with and without polarization for 5 days of cell differentiation under static and dynamic conditions.

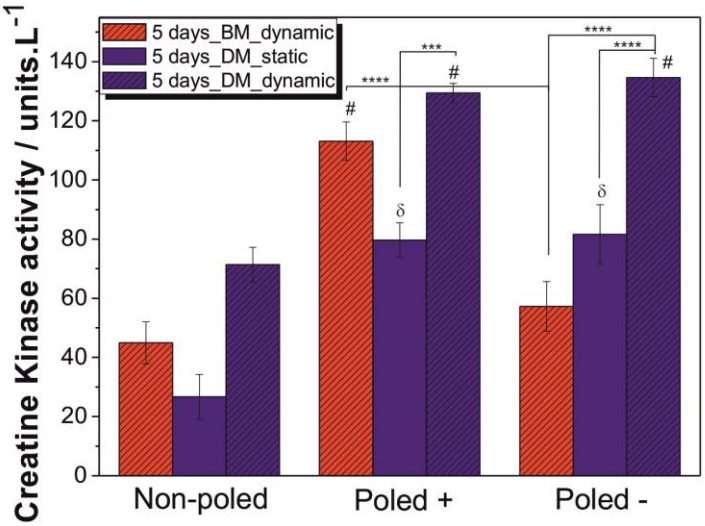


Figure 8 - Creatine kinase activity values after 5 days of C2C12 cell differentiation cultured on the different CFO/P(VDF-TrFE) samples: non-poled, "poled +" and "poled –". All the values are presented as average ± s.e.m. $^{***}p \leq 0.001$, $^{****}p \leq$

0.0001; $^{\delta}p \leq 0.01$ *vs* non-poled with BM and dynamic conditions and $^{\#}p \leq 0.0001$ *vs* non-poled with BM and dynamic conditions.

Comparing the static and dynamic conditions with DM it is evident that the samples cultured under dynamic conditions yield the highest values of creatine kinase activity. Further, the poled samples present higher values compared with the non-poled ones, being no significative differences among samples with different surface charge. Analyzing the samples under dynamic conditions but with and without DM, it is verified that no significant differences are obtained for non-poled and "poled +" samples, contrary to the "poled -" samples, where significant differences are observed, with higher values with DM. Once, as already stated before, the creatine kinase values are associated to the more mature myotubes. Thus, it is verified that these results are in agreement with the values of the maturation index (figure 7c).

The study of cell differentiation was kept up to 8 days and after this time, immunofluorescence staining of myosin heavy chain was investigated (figure 9).

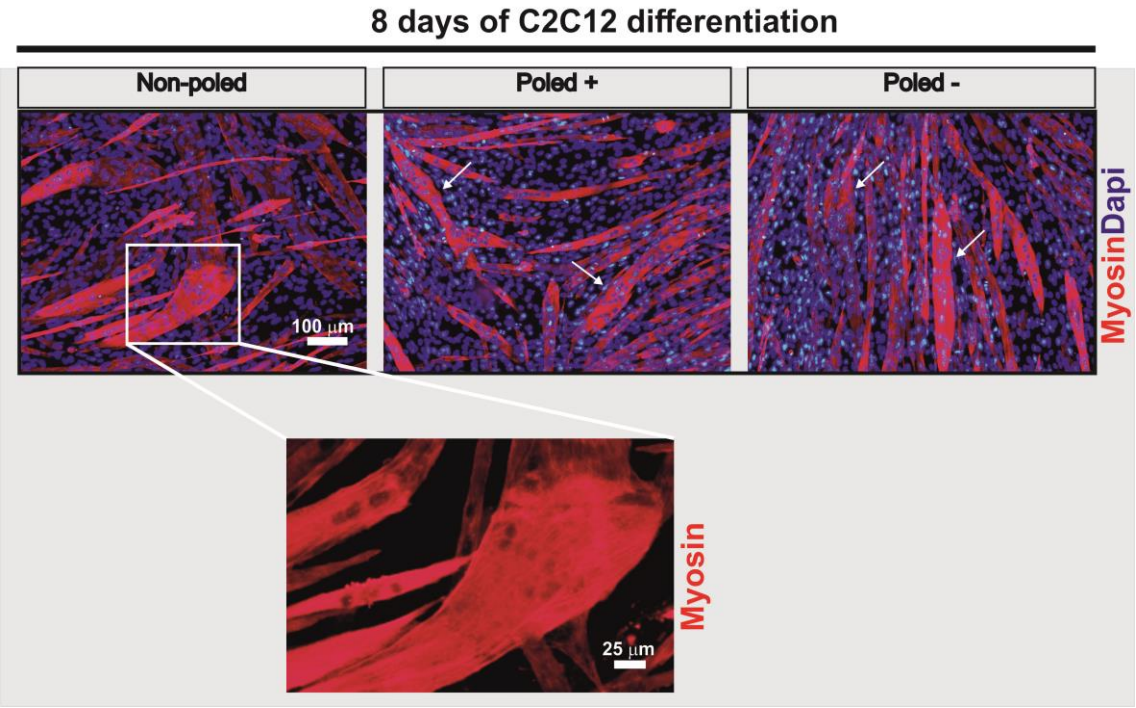


Figure 9 - Immunofluorescence microscopy images of C2C12 myoblast differentiated on different CFO/P(VDF-TrFE) films for 8 days with BM under dynamic conditions. Myotubes were fixed and stained with a MHC-specific antibody (red) and the nuclei counterstained with DAPI (blue). Scale bars represent 100 µm for all upper images.

Figure 9 shows the immunofluorescent staining of MHC images of C2C12 myoblast cells differentiated under dynamic conditions (magnetic stimulation) with BM. After 8 days of differentiation, it is verified that myotubes continue to grow with the same profile obtained after 5 days of differentiation, i.e just more mature myotubes are observed in all the samples when compared with the same sample and conditions. Namely, it is observed higher myotubes diameter on the non-poled samples and higher length in the poled ones. The same behavior was observed for the others conditions (data not shown), with similar differences between the samples and conditions observed after 5 days of differentiation.

Observing all the results obtained after evaluation of the influence of the surface charge (polarization) of the biomaterial and the stimuli provided to the cells (mechanical and/or electrical), it can be concluded that the polarization and also these stimuli enhance the myoblast differentiation, leading to more mature myotubes. Also, comparing the poled samples, it is verified that when only the physical stimuli was provided (BM at dynamic conditions), the samples with positive polarization

lead to significantly higher fusion and maturation index. This can be related to the fact that the cellular plasma membrane presents a negative charge [40]. Also, it has been demonstrated that the positive and negative charge can enhance/inhibit different phases of cell behavior. For example, the use of positive charged nanoparticles has demonstrated to inhibit stem cell proliferation but not differentiation [41]. However, when the physical stimulus is combined with the chemical one (DM), no significant differences are observed between cell culture on samples with different surface polarization.

Another important parameter for skeletal muscle TE is the alignment of the cells. This is important once the natural skeletal muscle presents a highly organized structure, with long parallel bundles of multinucleated myotubes. Besides that, a non-proper myotube alignment leads to an ineffective force transmission and contractility for regeneration of functional muscle fibers [42].

In this way, it is important the biomaterials to prevent random fusion and to lead to a proper elongation and alignment of myotubes. The fused myotubes formed in the different samples at different conditions have been this studied (Figure 10).

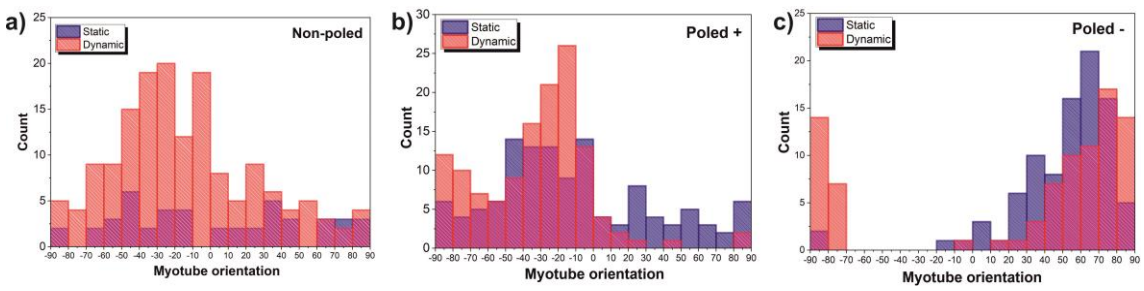


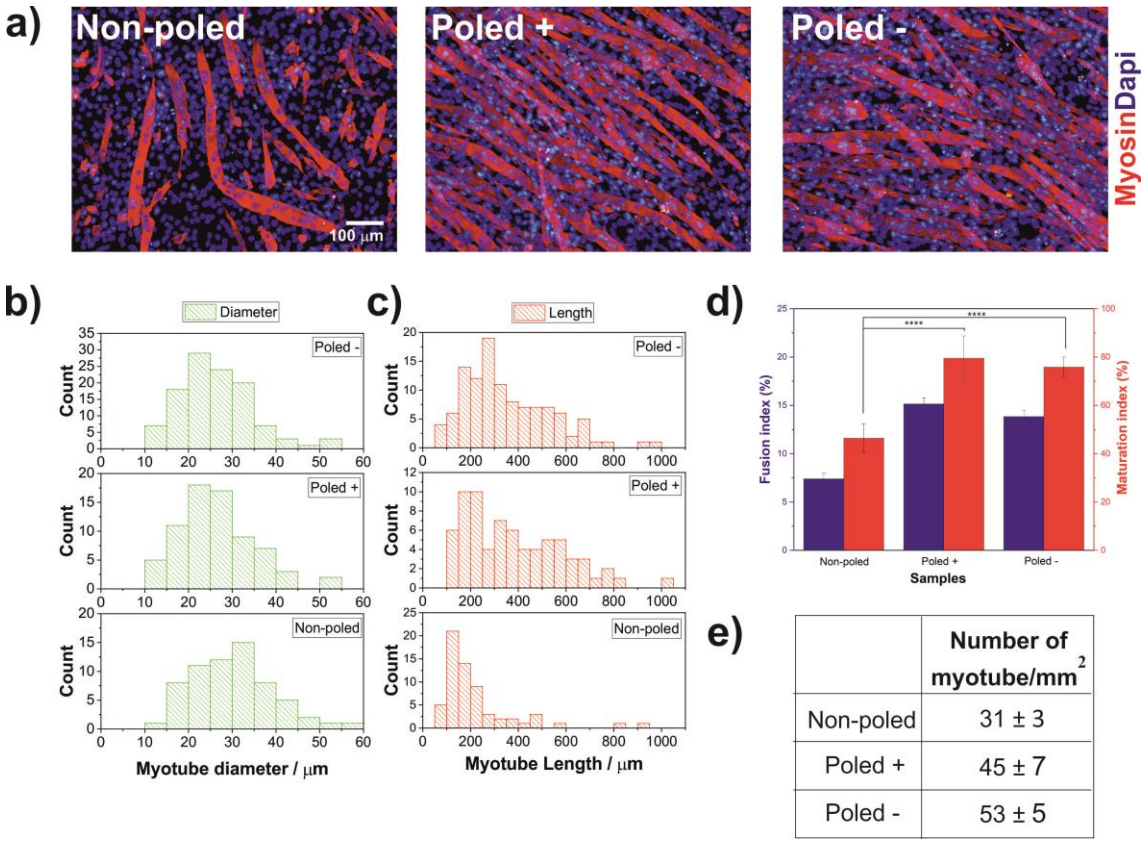
Figure 10 - Distribution of myotube orientation on the different CFO/P(VDF-TrFE) samples: (a) non-poled, (b) "poled +" and (c) "poled –"; with DM under static and dynamic conditions after 5 days of differentiation.

Regarding the distribution of myotube orientation on the different CFO/P(VDF-TrFE) samples, the polarization of the samples seems to induce some myotube orientation. When the mechanical and/or electrical stimuli are provided, it is verified that these stimuli induce the myotube orientation in all the samples; being more evident on the non-poled samples compared with the static conditions where

no myotube orientation was verified. Therefore, these results demonstrate that, together with the enhancement of myoblast differentiation, the developed materials lead to the myotubes alignment. In this way, magnetoelectric biomaterials show strong potential to be used for skeletal muscle TE. Therefore, this effect can be combined also with scaffolds with fibrillar morphology [43] which as has been shown strengthens the alignment of myotubes [13].

The previous results thus demonstrated that the mechano-electrical stimuli (provided by the magnetic home-made bioreactor) have large influence on proper C2C12 differentiation. However, it is possible to directly mechanically stimulate these magnetoelectric samples [24] with a home-made vibration bioreactor (see figure 1), obtaining a mechanically activated electroactive microenvironment. With this bioreactor a direct mechanical stimulation of the materials is provided, evaluating directly the piezoelectric response. Thus, studying this two kind of stimulation by different bioreactors, it is possible prove the positive influence of mechano-electric stimuli on the cells by two different approaches (magnetoelectric stimulation and direct piezoelectric stimulation). The study in this mechanical home-made bioreactor was performed with different CFO/P(VDF-TrFE) samples and no chemical stimuli (BM), for 5 days of cell differentiation, in order to evaluate and compare only the physical stimuli.

The figure 11 shows the immunofluorescent images and some myotube quantitative parameters obtained on the CFO/P(VDF-TrFE) samples with BM under dynamic conditions through the use of the mechanical home-made bioreactor.



	Number of myotube/mm^2
Non-poled	31 ± 3
Poled +	45 ± 7
Poled -	53 ± 5

Figure 11 - (a) Immunofluorescent staining of myosin heavy chain (MHC) after 5 days of C2C12 cells differentiation under dynamic condition (mechanical stimulation) with BM on the different CFO/P(VDF-TrFE) samples. Scale bars represent 100 µm for all images. Quantification of (b) myotube diameter, (c) myotube length, (d) fusion and maturation index and (e) number of myotubes/mm^2. Data are expressed as the mean ± s.e.m., $^{****}p \leq 0.0001$.

Figure 11a shows that all materials under mechanical stimulation promote C2C12 differentiation, where the electrically charged materials lead to higher fusion and maturation index values (Figure 11d) than samples without charge (non-poled), in which just mechanical and not mechano-electric stimulation occurs. It is to notice that these results are fully in agreement with the ones obtained with the magnetic home-made bioreactor.

Also, no significant differences between samples cultured on "poled +" and "poled –" samples were obtained. The size of myotubes, more specifically their length (figure 11c) and diameter (figure 11b) shows that higher values of maturation index are also associated with longer myotubes. The "poled +" CFO/(PVDF-TrFE) samples support the biggest myotubes with 391.05 ± 34.19 µm, with no significant differences compared to the "poled –", ≈ 356.28 ± 24.34 µm. Relatively to the distribution of the myotube diameter (figure 11b), it is observed that the diameter average values obtained for all

samples ranged between 26.38 ± 1.04 and 30.50 ± 1.18 μm, with the non-poled samples leading to the largest diameter. Myotube number was also quantified (figure 11e) and the results demonstrate that the mechano-electrical stimulus promotes higher differentiation, and consequently, higher myotube formation, with no significative differences between both polarization states, 45 ± 7 and 53 ± 5, for "poled +" and "poled –", respectively.

The use of a home-made bioreactor system with mechanical solicitations at 1 Hz confirmed the relevance of the mechano-electric stimuli for muscle differentiation. With this approach (direct mechanical stimuli), higher values of electrical stimuli (64 μV) are provided (as calculated from the piezoelectric coefficient of the materials) to the cells.

An overview of the cell response obtained by the use of the different home-made bioreactors are compared in Table 2, showing the data of the fusion and maturation index obtained in the different samples with BM at static and dynamic conditions in the two bioreactors.

Table 2 – Quantitative comparison of MHC among the different samples after 5 days of differentiation under static and dynamic (magnetic and mechanical stimulation) conditions.

Conditions	Medium	Bioreactor Stimulus	Samples	Fusion index	Maturation index
Static	BM	-------	Non-poled	3.78 ± 0.51	12.73 ± 2.96
			Poled +	9.59 ± 0.13	37.52 ± 4.01
			Poled -	4.9 ± 0.1	34.59 ± 2.72
Dynamic		Magnetic	Non-poled	7.17 ± 0.24	32.85 ± 3.90
			Poled +	17.03 ± 0.89	68.88 ± 2.67
			Poled -	11.15 ± 0.60	44.24 ± 3.49
		Mechanical	Non-poled	7.38 ± 0.58	46.41 ± 5.97
			Poled +	15.14 ± 0.95	79.52 ± 11.23
			Poled -	13.83 ± 0.73	75.88 ± 4.17

Regarding the table 2, it is verified that the fusion and maturation index values are slightly higher with direct mechanical stimulation. Once the values of electrical stimuli provided by this bioreactor are superior to those provided by the magnetic one, it is concluded than the mechanical but mostly the electrical cues, play a key role on muscle differentiation. In this way, electromechanical microenvironments, either directly mechanically or magnetically activated show an excellent potential for skeletal muscle TE, by providing the necessary physical stimuli present in the natural tissue in the human body.

4-Conclusions

This work demonstrates the relevance of electromechanically active microenvironments for muscle tissue engineering. The mechanical and electrical activation of the microenvironment has been

performed either directly (direct application of mechanical solicitation to produce the piezoelectric response of the material) or indirectly (magnetically activated) by using magnetoelectric biomaterials - that allows triggering cellular response by non-contact external stimulation. Herein, the suitability of the magnetoelectric effect for skeletal muscle tissue engineering was demonstrated with CFO/P(VDF-TrFE) films with different surface charges. These biomaterials allowed mechanical (0.013 $\mu m.mm^{-2}$) and electrical (16.15 μV and 64 μV, thought magnetic an mechanical bioreactor, respectively) stimulation of the cells. Relatively to the myogenic cell differentiation, this study showed that at dynamic conditions, the application of mechanical (non-poled samples) and mechano-electrical ("poled +" and "poled -" samples) stimuli promote the C2C12 cells differentiation (higher presence of MHC) comparatively to the static conditions. As verified in the cell proliferation, charged samples show higher maturation index, with no significant differences in positive and negatively charged surfaces. A magnetically or mechanically activated electroactive microenvironment was provided to the cells by the use of a magnetic or mechanical bioreactor, respectively. Comparing both stimulation procedures, it is concluded that the mechanical but mostly the electrical cues play a key role on muscle differentiation. Concluding, this study proves the need of biomimetic electroactive microenvironments for muscle tissue engineering and demonstrated how to apply these stimuli remotely by magnetoelectric biomaterials.

Acknowledgments

This work was supported by the Portuguese Foundation for Science and Technology (FCT) in the framework of the Strategic Funding UID/FIS/04650/2020, UID/BIA/04050/2020, UID/BIO/04469/2020 and projects PTDC/BTM-MAT/28237/2017 and PTDC/EMD-EMD/28159/2017. The authors also thank the FCT for the SFRH/BD/111478/2015 (S.R.) grant. The authors acknowledge funding by the Spanish Ministry of Economy and Competitiveness (MINECO)

through the project MAT2016-76039-C4-3-R (AEI/FEDER, UE) and from the Basque Government Industry and Education Department under the ELKARTEK, HAZITEK and PIBA (PIBA-2018-06) programs, respectively.

Data availability statement

The data generated during the current study are available from the corresponding author on reasonable request.

References

(1) Meyer, U.; Meyer, T.; Handschel, J.; Wiesmann, H. P. *Fundamentals of tissue engineering and regenerative medicine*, 2009; p 1-1049.
(2) Tabebordbar, M.; Wang, E. T.; Wagers, A. J., Skeletal muscle degenerative diseases and strategies for therapeutic muscle repair. In *Annual Review of Pathology: Mechanisms of Disease*, 2013; Vol. 8, pp 441-475.
(3) Frontera, W. R.; Ochala, J. Skeletal Muscle: A Brief Review of Structure and Function. *Behavior Genetics* **2015,** *45* (2), 183-195, DOI: 10.1007/s00223-014-9915-y.
(4) Nakayama, K. H.; Shayan, M.; Huang, N. F. Engineering Biomimetic Materials for Skeletal Muscle Repair and Regeneration. *Advanced Healthcare Materials* **2019,** *8* (5), DOI: 10.1002/adhm.201801168.
(5) Guiraud, S.; Davies, K. E. Regenerative biomarkers for Duchenne muscular dystrophy. *Neural Regeneration Research* **2019,** *14* (8), 1317-1320, DOI: 10.4103/1673-5374.253534.
(6) Shafiee, A.; Atala, A., Tissue Engineering: Toward a New Era of Medicine. In *Annual Review of Medicine*, 2017; Vol. 68, pp 29-40.
(7) Pérez, R. A.; Won, J. E.; Knowles, J. C.; Kim, H. W. Naturally and synthetic smart composite biomaterials for tissue regeneration. *Advanced Drug Delivery Reviews* **2013,** *65* (4), 471-496, DOI: 10.1016/j.addr.2012.03.009.
(8) Rangarajan, S.; Madden, L.; Bursac, N. Use of flow, electrical, and mechanical stimulation to promote engineering of striated muscles. *Annals of Biomedical Engineering* **2014,** *42* (7), 1391-1405, DOI: 10.1007/s10439-013-0966-4.
(9) Dao, T. T.; Tho, M. C. H. B. A systematic review of continuum modeling of skeletal muscles: Current trends, limitations, and recommendations. *Applied Bionics and Biomechanics* **2018,** *2018*, DOI: 10.1155/2018/7631818.
(10) Liao, I. Effect of Electromechanical Stimulation on the Maturation of Myotubes on Aligned Electrospun Fibers. *Cellular and Molecular Bioengineering* **2008,** *1* (2-3), 133145.
(11) Ribeiro, C.; Sencadas, V.; Correia, D. M.; Lanceros-Méndez, S. Piezoelectric polymers as biomaterials for tissue engineering applications. *Colloids and Surfaces B: Biointerfaces* **2015,** *136*, 46-55, DOI: 10.1016/j.colsurfb.2015.08.043.
(12) Martins, P. M.; Ribeiro, S.; Ribeiro, C.; Sencadas, V.; Gomes, A. C.; Gama, F. M.; Lanceros-Méndez, S. Effect of poling state and morphology of piezoelectric poly(vinylidene fluoride) membranes for skeletal muscle tissue engineering. *RSC Advances* **2013,** *3* (39), 17938-17944, DOI: 10.1039/c3ra43499k.
(13) Ribeiro, S.; Gomes, A. C.; Etxebarria, I.; Lanceros-Méndez, S.; Ribeiro, C. Electroactive biomaterial surface engineering effects on muscle cells differentiation. *Materials Science and Engineering C* **2018,** *92*, 868-874, DOI: 10.1016/j.msec.2018.07.044.

(14) Cardoso, V. F.; Correia, D. M.; Ribeiro, C.; Fernandes, M. M.; Lanceros-Méndez, S. Fluorinated polymers as smart materials for advanced biomedical applications. *Polymers* **2018,** *10* (2), DOI: 10.3390/polym10020161.
(15) Koppes, R. A.; Schiele, N. R.; Corr, D. T. In *An electromechanical bioreactor for scaffold-free skeletal muscle tissue engineering*, ASME 2011 Summer Bioengineering Conference, SBC 2011, 2011; pp 135-136.
(16) Gazendam, M. G. J.; Hof, A. L. Averaged EMG profiles in jogging and running at different speeds. *Gait and Posture* **2007,** *25* (4), 604-614, DOI: 10.1016/j.gaitpost.2006.06.013.
(17) Sasaki, K.; Neptune, R. R. Muscle mechanical work and elastic energy utilization during walking and running near the preferred gait transition speed. *Gait and Posture* **2006,** *23* (3), 383-390, DOI: 10.1016/j.gaitpost.2005.05.002.
(18) Dong, R.; Ma, P. X.; Guo, B. Conductive biomaterials for muscle tissue engineering. *Biomaterials* **2020,** *229*, DOI: 10.1016/j.biomaterials.2019.119584.
(19) Dobson, J. Remote control of cellular behaviour with magnetic nanoparticles. *Nature Nanotechnology* **2008,** *3* (3), 139-143, DOI: 10.1038/nnano.2008.39.
(20) Ribeiro, C.; Correia, V.; Martins, P.; Gama, F. M.; Lanceros-Mendez, S. Proving the suitability of magnetoelectric stimuli for tissue engineering applications. *Colloids and Surfaces B: Biointerfaces* **2016,** *140*, 430-436, DOI: 10.1016/j.colsurfb.2015.12.055.
(21) Martins, P.; Lasheras, A.; Gutierrez, J.; Barandiaran, J. M.; Orue, I.; Lanceros-Mendez, S. Optimizing piezoelectric and magnetoelectric responses on CoFe <inf>2</inf>O<inf>4</inf>/P(VDF-TrFE) nanocomposites. *Journal of Physics D: Applied Physics* **2011,** *44* (49), DOI: 10.1088/0022-3727/44/49/495303.
(22) Martins, P.; Lasheras, A.; Gutierrez, J.; Barandiaran, J. M.; Orue, I.; Lanceros-Mendez, S. Optimizing piezoelectric and magnetoelectric responses on CoFe <inf>2</inf> O <inf>4</inf> /P(VDF-TrFE) nanocomposites. *Journal of Physics D: Applied Physics* **2011,** *44* (49), DOI: 10.1088/0022-3727/44/49/495303.
(23) Ribeiro, C.; Costa, C. M.; Correia, D. M.; Nunes-Pereira, J.; Oliveira, J.; Martins, P.; Gonçalves, R.; Cardoso, V. F.; Lanceros-Méndez, S. Electroactive poly(vinylidene fluoride)-based structures for advanced applications. *Nature Protocols* **2018,** *13* (4), 681-704, DOI: 10.1038/nprot.2017.157.
(24) Ribeiro, C.; Moreira, S.; Correia, V.; Sencadas, V.; Rocha, J. G.; Gama, F. M.; Gómez Ribelles, J. L.; Lanceros-Méndez, S. Enhanced proliferation of pre-osteoblastic cells by dynamic piezoelectric stimulation. *RSC Advances* **2012,** *2* (30), 11504-11509, DOI: 10.1039/c2ra21841k.
(25) Ribeiro, C.; Pärssinen, J.; Sencadas, V.; Correia, V.; Miettinen, S.; Hytönen, V. P.; Lanceros-Méndez, S. Dynamic piezoelectric stimulation enhances osteogenic differentiation of human adipose stem cells. *Journal of Biomedical Materials Research - Part A* **2015,** *103* (6), 2172-2175, DOI: 10.1002/jbm.a.35368.
(26) Prabhakaran, T. a. H., J. Poly(vinylidene fluoride)-Based Magnetoelectric Polymer Nanocomposite Films. In *Magnetoelectric Polymer-Based Composites*; P.Martins, e. S. L.-M. a., Ed.; 2017; pp 87-113.
(27) Martins, P.; Lopes, A. C.; Lanceros-Mendez, S. Electroactive phases of poly(vinylidene fluoride): Determination, processing and applications. *Progress in Polymer Science* **2014,** *39* (4), 683-706, DOI: 10.1016/j.progpolymsci.2013.07.006.
(28) Correia, D. M.; Nunes-Pereira, J.; Alikin, D.; Kholkin, A. L.; Carabineiro, S. A. C.; Rebouta, L.; Rodrigues, M. S.; Vaz, F.; Costa, C. M.; Lanceros-Méndez, S. Surface wettability modification of poly(vinylidene fluoride) and copolymer films and membranes by plasma treatment. *Polymer* **2019,** *169*, 138-147, DOI: 10.1016/j.polymer.2019.02.042.
(29) Gonçalves, R.; Martins, P.; Correia, D. M.; Sencadas, V.; Vilas, J. L.; León, L. M.; Botelho, G.; Lanceros-Méndez, S. Development of magnetoelectric CoFe<inf>2</inf>O<inf>4</inf> /poly(vinylidene fluoride) microspheres. *RSC Advances* **2015,** *5* (45), 35852-35857, DOI: 10.1039/c5ra04409j.
(30) Yuan, Y.; Lee, T. R., Contact angle and wetting properties. In *Springer Series in Surface Sciences*, 2013; Vol. 51, pp 3-34.
(31) Ribeiro, C.; Panadero, J. A.; Sencadas, V.; Lanceros-Méndez, S.; Tamaño, M. N.; Moratal, D.; Salmerón-Sánchez, M.; Gómez Ribelles, J. L. Fibronectin adsorption and cell response on electroactive poly(vinylidene fluoride) films. *Biomedical Materials* **2012,** *7* (3), DOI: 10.1088/1748-6041/7/3/035004.
(32) Serrado Nunes, J.; Wu, A.; Gomes, J.; Sencadas, V.; Vilarinho, P. M.; Lanceros-Méndez, S. Relationship between the microstructure and the microscopic piezoelectric response of the α- And β-phases of

poly(vinylidene fluoride). *Applied Physics A: Materials Science and Processing* **2009,** *95* (3), 875-880, DOI: 10.1007/s00339-009-5089-2.
(33) Ranella, A.; Barberoglou, M.; Bakogianni, S.; Fotakis, C.; Stratakis, E. Tuning cell adhesion by controlling the roughness and wettability of 3D micro/nano silicon structures. *Acta Biomaterialia* **2010,** *6* (7), 2711-2720, DOI: 10.1016/j.actbio.2010.01.016.
(34) Webb, K.; Hlady, V.; Tresco, P. A. Relative importance of surface wettability and charged functional groups on NIH 3T3 fibroblast attachment, spreading, and cytoskeletal organization. *Journal of Biomedical Materials Research* **1998,** *41* (3), 422-430, DOI: 10.1002/(sici)1097-4636(19980905)41:3<422::aid-jbm12>3.0.co;2-k.
(35) Ribeiro, C.; Sencadas, V.; Areias, A. C.; Gama, F. M.; Lanceros-Méndez, S. Surface roughness dependent osteoblast and fibroblast response on poly(L-lactide) films and electrospun membranes. *Journal of Biomedical Materials Research - Part A* **2015,** *103* (7), 2260-2268, DOI: 10.1002/jbm.a.35367.
(36) Metwally, S.; Stachewicz, U. Surface potential and charges impact on cell responses on biomaterials interfaces for medical applications. *Materials Science and Engineering C* **2019,** *104*, DOI: 10.1016/j.msec.2019.109883.
(37) Bays, J. L.; DeMali, K. A. Vinculin in cell–cell and cell–matrix adhesions. *Cellular and Molecular Life Sciences* **2017,** *74* (16), 2999-3009, DOI: 10.1007/s00018-017-2511-3.
(38) Parssinen, J.; Hammarén, H.; Rahikainen, R.; Sencadas, V.; Ribeiro, C.; Vanhatupa, S.; Miettinen, S.; Lanceros-Méndez, S.; Hytönen, V. P. Enhancement of adhesion and promotion of osteogenic differentiation of human adipose stem cells by poled electroactive poly(vinylidene fluoride). *Journal of Biomedical Materials Research - Part A* **2015,** *103* (3), 919-928, DOI: 10.1002/jbm.a.35234.
(39) Chal, J.; Pourquié, O. Making muscle: Skeletal myogenesis in vivo and in vitro. *Development (Cambridge)* **2017,** *144* (12), 2104-2122, DOI: 10.1242/dev.151035.
(40) Chen, Y. S.; Harn, H. J.; Chiou, T. W. The Role of Biomaterials in Implantation for Central Nervous System Injury. *Cell Transplantation* **2018,** *27* (3), 407-422, DOI: 10.1177/0963689717732991.
(41) Li, J. J.; Kawazoe, N.; Chen, G. Gold nanoparticles with different charge and moiety induce differential cell response on mesenchymal stem cell osteogenesis. *Biomaterials* **2015,** *54*, 226-236, DOI: 10.1016/j.biomaterials.2015.03.001.
(42) Jana, S.; Levengood, S. K. L.; Zhang, M. Anisotropic Materials for Skeletal-Muscle-Tissue Engineering. *Advanced Materials* **2016,** *28* (48), 10588-10612, DOI: 10.1002/adma.201600240.
(43) Maciel, M. M.; Ribeiro, S.; Ribeiro, C.; Francesko, A.; Maceiras, A.; Vilas, J. L.; Lanceros-Méndez, S. Relation between fiber orientation and mechanical properties of nano-engineered poly(vinylidene fluoride) electrospun composite fiber mats. *Composites Part B: Engineering* **2018,** *139*, 146-154, DOI: 10.1016/j.compositesb.2017.11.065.